Article

Capacitive Model for Coulometric Readout of Ion-Selective Electrodes

JAROLIMOVA, Zdenka, *et al*.

Abstract

We present here a capacitive model for the coulometric signal transduction readout of solid-contact ionselective membrane electrodes (SC-ISE) with a conducting polymer (CP) as an intermediate layer for the detection of anions. The capacitive model correlates well with experimental data obtained for chloride-selective SC-ISEs utilizing poly(3,4-ethylenedioxythiophene) (PEDOT) doped with chloride as the ion-to-electron transducer. Additionally, Prussian blue is used as a simple sodium capacitor to further demonstrate the role of the transduction layer. The influence of different thicknesses of PEDOT as a conducting polymer transducer, different thicknesses of the overlaying ion-selective membranes deposited by drop casting and spin coating, and different compositions of the chloride-selective membrane are explored. The responses are evaluated in terms of current−time, charge−time, and charge−chloride activity relationships. The utility of the sensor with coulometric readout is illustrated by the monitoring of very small concentration changes in solution.

Reference

JAROLIMOVA, Zdenka, *et al*. Capacitive Model for Coulometric Readout of Ion-Selective Electrodes. *Analytical Chemistry*, 2018, vol. 90, no. 14, p. 8700-8707

DOI : 10.1021/acs.analchem.8b02145

Capacitive Model for Coulometric Readout of Ion-Selective Electrodes

Zdeňka Jarolímová,[a] Tingting Han,[b] Ulriika Mattinen,[b] Johan Bobacka,[b*] and Eric Bakker [a*]

Post-review print

Jarolimova, Z.; Han, T.; Mattinen, U.; Bobacka, J.; Bakker, E. “Capacitive Model for Coulometric Readout of Ion-Selective Electrodes”, Anal. Chem. **2018**, *90*, 8700-8707.

DOI: 10.1021/acs.analchem.8b02145

Capacitive Model for Coulometric Readout of Ion-Selective Electrodes

Zdeňka Jarolímová,[a] Tingting Han,[b] Ulriika Mattinen,[b] Johan Bobacka,[b*] and Eric Bakker [a*]

[a] Department of Inorganic and Analytical Chemistry, University of Geneva, Quai Ernest Ansermet 30, 1211 Geneva 4 (Switzerland)

[b] Johan Gadolin Process Chemistry Centre, Laboratory of Analytical Chemistry, Åbo Akademi University, Biskopsgatan 8, FI-20500 Turku-Åbo (Finland)

KEYWORDS: constant-potential coulometry, capacitor, ion-selective membrane electrodes.

ABSTRACT: We present here a capacitive model for the coulometric signal transduction readout of solid-contact ion-selective membrane electrodes (SC-ISE) with a conducting polymer (CP) as an intermediate layer for the detection of anions. The capacitive model correlates well with experimental data obtained for chloride-selective SC-ISE utilizing poly(3,4-ethylenedioxythiophene) (PEDOT) doped with chloride as the ion-to-electron transducer. Additionally, Prussian blue is used as a simple sodium capacitor to further demonstrate the role of the transduction layer. The influence of different thicknesses of PEDOT as a conducting polymer transducer, different thicknesses of the overlaying ion-selective membranes deposited by drop casting and spin coating, and different compositions of the chloride-selective membrane are explored. The responses are evaluated in terms of current–time, charge–time and charge–chloride activity relationships. The utility of the sensor with coulometric readout is illustrated by the monitoring of very small concentration changes in solution.

Polymeric ion selective membranes (ISMs) are important electrochemical sensors in fundamental science, as well as in applied work such as pharmaceutical industry, clinical diagnostic, environmental or forensic monitoring.[1-4] The exploration and the development of electrochemical sensors have been the subject of considerable interest and efforts in recent years and their application allows one to develop a new generation of ion sensors.

The field of electrochemical sensors has not only been focused on the development of new electrochemical sensors but also on the introduction of new fundamental sensing concepts, attractive methodologies and new ion-selective readout principles. Xie et al., based on earlier work by Wolfbeis, demonstrated that the potentiometric response of ion-selective nanospheres can be observed with voltage-sensitive dyes, where nanoscale electrochemical signals are converted into an optical readout.[5-7] The working mechanism is based on the distribution of solvatochromic dye between the aqueous and organic phases according to the Galvani potential and one may use fluorescence to read out concentration changes. Mikhelson et al. proposed an approach for sensing single-ion activities using ion optodes with lipophilic electrolyte to impose a constant phase boundary potential across the sample−membrane interface.[8] A new ion sensing platform for conversion of cell potentials from ion-selective electrodes to a light output to indicate the potential change has been reported in separate works by Crespo et al. (electrochemiluminescence) and by Zhang et al. (light emitting diodes).[9,10]

A potentially interesting way to read out ion-selective membranes is constant-potential coulometry, which has been recently introduced by Hupa et al.[11] The prerequisite for this methodology is an inner transducing layer playing the role of an ideal capacitor between the electrical conductor and the ion-selective membrane. A constant potential coulometry experiment uses the redox capacitance of the internal solid contact to convert a change in ion concentration (activity) into a transient current pulse whose charge serves as the analytical signal. This concept was originally introduced using a conducting polymer PEDOT doped with poly(styrenesulfonate) (PSS) as the redox capacitor but there are many other materials that can be used as inner transduction elements, including other conducting polymers (CPs), three-dimensionally ordered macro-porous (3DOM) carbon, carbon nanotubes (CNTs), fullerene, graphene, redox active monolayers and redox probes.[11-24] This coulometric signal readout method was extended and characterized in more detail by Vanamo et al. using different thicknesses of PEDOT(PSS) as solid contact covered with a potassium-selective membrane.[25] Furthermore, Han et al. reported on the influence of the electrode geometry on the response time of SC-ISEs based on a 1 mC film of PEDOT(PSS). It was shown that the response time of the coulometric readout is shortened significantly with increasing area of the ion-selective membrane electrode, i.e. with decreasing resistance of the electrode.[26] The chronopotentiometric response of cation-selective SC-ISEs based on PEDOT(PSS) as solid contact has been approximated earlier by Bobacka et al. utilizing a series resistor-capacitor (RC) equivalent circuit model.[12]

Our aim here is to establish a useful, simplified fundamental theoretical treatment of the coulometric transduction mechanism introduced recently for SC-ISEs.[11,25,26] The present work is focused on anion-selective SC-ISEs and accompanied with mathematical calculations. The theoretical model allows one to predict the transient current pulse, current amplitude, RC

time constant and the total cumulative charge in a wide concentration range of the analyte ion. The coulometric transduction method markedly increases the sensitivity of ion detection and allows one to measure very small changes in ion activity.

THEORETICAL MODEL

A membrane electrode containing a capacitive inner transducing layer is held at a constant potential and allowed to equilibrate so that the observed current is initially zero. An analyte activity change at time t_0 will result in a potential change at the membrane–sample boundary, ideally according to the Nernst equation:

$$\Delta E_{pb}(sample) = \frac{s}{z} log \frac{a_i(final)}{a_i(initial)} \quad (1)$$

Here, s is 59.2 mV for 25 °C and z_i is the charge of the analyte ion (anions have a negative value of z_i). In order to fulfill the value of the imposed potential, which remains indifferent, the change at the inner membrane side (inner transducing layer) must be exactly opposite this value:

$$\Delta E_{pb}(inner\ side) = slog \frac{a_i(initial)}{a_i(final)} \quad (2)$$

The resulting current response of the system is described in analogy to a constant potential step at a capacitor, which is written for the system under study as:

$$i(t) = \frac{\Delta E_{pb}(inner\ side)}{R_{cell}} e^{\frac{t-t_0}{C_{cp}R_{cell}}} \quad (3)$$

where C_{cp} is the capacitance of the inner transducing layer and R_{cell} is the resistance of the electrochemical cell. Equation 2 is inserted into eqn. 3 to find the relationship between current transient and activity change in the sample as follows (Figure S1A, S1B):

$$i(t) = \frac{s}{z_i R_{cell}} log \left(\frac{a_i(initial)}{a_i(final)}\right) e^{\frac{t-t_0}{C_{cp}R_{cell}}} \quad (4)$$

This transient describes a current peak at time t_0 that decays with a time constant RC that is a function of the capacitance of the conducting polymer and the cell resistance. Ion-selective membranes that are more resistive will result in larger time constants (increasing R_{cell}) and hence lower possible sampling frequencies. Of course, mass transport across the membrane triggered by the current transient may also be limiting the overall time response, and for this reason as well thinner membranes are expected to be advantageous.

The peak current is found at t_0 as:

$$i_p = \frac{s}{z_i R_{cell}} log \left(\frac{a_i(initial)}{a_i(final)}\right) \quad (5)$$

It is evident that the magnitude of the peak current not only depends on the Nernst function, but also on the cell resistance. If the membrane resistance does not dominate the cell resistance this may result in possible uncertainties in the measurement.

To overcome this potential limitation, the current may be integrated over time to give the following relationship between observed charge and concentration change (Figure S1C), which is now independent of resistance:

$$Q_p = C_{cp} \frac{s}{z_i} log \left(\frac{a_i(initial)}{a_i(final)}\right) \quad (6)$$

The observed charge should linearly depend on the logarithmic activity change in the sample, giving a negative slope of $-C_{cp}\ s\ /\ z_i$ for cations and one of positive sign for anions. The integrated charge depends linearly on the capacitance of the inner transducing layer. A higher capacitance should result in a larger charge, but at the price of a larger time constant and therefore a slower recovery of the current spike. The predictions of this theory is in good qualitative agreement with earlier experimental findings for K^+-selective SC-ISEs utilizing coulometric readout.[25,26]

EXPERIMENTAL SECTION

Reagents and solutions. Potassium chloride (KCl), sodium chloride (NaCl), tridodecylmethylammonium chloride (TDMACl), poly(vinyl chloride) of high molecular weight (PVC), nitrophenyloctyl ether (NPOE), 4,5-Dimethyl-3,6-dioctyloxy-o-phenylene-bis(mercurytrifluoroacetate) (chloride ionophore II, ETH 9009), tetrakis(4-chlorophenyl)borate tetradodecylammonium salt (ETH 500, R^+R^-), tetrahydrofuran (THF), 3,4-ethylendioxythiophene (EDOT, 97%) were obtained from Sigma Aldrich.

Instrumentation and measurements. Working electrodes of (3.0 ± 0.1) mm electrode diameter (7.06 mm^2 geometric surface area) were prepared by inserting a glassy carbon rod (GC, Sigradur G, HTW Hochtemperatur − Werkstoffe GmbH, D-86672, Thierhaupten, Germany) into a PVC housing. A GC rod (3.2 cm^2 surface area) was used as a counter electrode. A double - junction Ag/AgCl/3M KCl/0.1M KCl reference electrode was used in chronoamperometric and potentiometric measurements (Metrohm Autolab, Utrecht, The Netherlands). The electropolymerization was performed galvanostatically in a conventional three-electrode cell using an Autolab General Purpose Electrochemical System (Metrohm Autolab Aut30.FRA2, Eco Chemie, B.V., The Netherlands). The open circuit potential (OCP) was determined prior the chronoamperometric measurements. The chronoamperometric measurements were performed with an Iviumstat (Ivium Technologies, The Netherlands) by using a conventional three electrodes cell. In order to reduce the background drift and obtain stable current smaller than 1 nA, the electrode were allowed to equilibrate in the measurement electrolyte at the open circuit potential before starting the dilution procedure as it gives the shortest equilibration time.[25] Potentiometric calibrations were performed with a multichannel meter (Lawson EMF16 interface potentiometer, Lawson Laboratories, Inc.). The automatic dilution was performed with a 765-automatic Dosimat (Metrohm Autolab, Utrecht). The pumping program controlled the dilution, 34.2 mL of electrolyte was pumped out of the starting volume 100 mL and replaced with an equivalent volume of Mili-Q water (0.18 decades/dilution step). Electrochemical impedance spectra (EIS) for the SC-ISEs with different polymerization charge of PEDOT(Cl) were measured in 10 mM KCl at open circuit potential (OCP) by an Autolab General Purpose Electrochemical System (Metrohm Autolab Aut30.FRA2, Eco Chemie, B.V., The Netherlands). The frequency range was 100 kHz – 10 mHz and the excitation amplitude was 10 mV. The thin membrane film was spin coated on the electrode using a special holder on a spin coater at 1500 rpm.

Electrode preparation. The polymerization solution (0.01 M EDOT and 0.1 M KCl) was left to stir overnight to ensure proper dissolution of the monomer. Prior to polymerization, the solution was deaerated by nitrogen flow for 20 min, after which nitrogen was positioned to flow above the solution to prevent interference from oxygen. PEDOT(Cl) films of different thicknesses were prepared by applying 0.2 mA cm^{-2} current for 71, 143, 286 and 714 s to obtain films with 1 mC, 2 mC, 4 mC and 10 mC total charge, respectively. Galvanostatic

deposition of the conducting polymer enables precise control of the polymerization charge and thus the redox capacitance of the PEDOT(Cl) layer.[12,27] After polymerization, the GC/PEDOT(Cl) electrodes were rinsed with deionized water, and allowed to dry in air for 1 day. Then, 60, 50 and 15 µL of anion-selective membrane cocktail was drop-casted or 25 µL of anion-selective membrane cocktail was spin-coated on each electrode at 1500 rpm. The thin membrane was spin coated onto the GC electrode by casting a volume of 25 µL of the cocktail with a spinning time of 2 min at 1500 rpm. Deposition of the Prussian blue (PB) film was accomplished in a solution of 10 mM $K_3[Fe(CN)_6]$, 10 mM $FeCl_3$ and 100 mM KCl. Applying a constant potential of 0.0 V to the polished glassy carbon electrode for 60 s, and then scanning 10 cycles at a sweep rate of 50 mV s^{-1} between 0.0 and 0.5 V formed a Prussian blue film.[28]

Composition of membrane cocktails. The final composition of chloride-selective membranes is shown in Table 1. All components for drop-cast membranes were dissolved in 1 mL of THF. All components (total mass of 50 mg) for spin-coated membranes were dissolved in 2 mL of THF according to the procedure described elsewhere.[29-31] THF was used to enhance the solubility of the compounds in the plasticizer. After evaporation of THF, the anion - selective SC-ISEs were conditioned in 0.1 M KCl for potentiometric measurements and in 0.01 M KCl for chronoamperometric measurements for 2 days.

RESULTS AND DISCUSSIONS

As described in the theoretical section, one may predict the experimental behavior of a capacitive inner transducing layer (the transient current pulse, current amplitude, a RC time constant and the total cumulative charge) as a function of thickness of the intermediate layer, the membrane thickness and the membrane composition. A proposed working mechanism of the transduction process for a simple capacitor is schematically illustrated in Figure 1. Any change in the ion activity in a bulk sample solution (s) results in a potential change at the phase boundary (pb). Since the system is held at a constant potential, any change in ion activity will result in a transient current associated with charging/discharging of the capacitor that in turn causes a potential change of the capacitor (TL). Figure 2 shows schematically how the capacitances and cell resistances influence the current peak and the charge. Figure 3 gives the theoretical dependence of the current amplitude and integrated charge on the capacitance of the transducing layer C_{cp} and the cell resistance R_{cell}. Figure 3A shows the transient current changes for a sample concentration change at time t_0. The current transient decays with a time constant RC, a function of the capacitance of the transducing layer C_{cp} and the cell resistance R_{cell}. Figure 3B shows cumulative charge integrated from the current over time for a given concentration change, which is a function of capacitance. If one keeps the membrane thickness constant and only vary the thickness of the transducing layer (and as a consequence the resulting capacitance), the peak current amplitude should not change with increasing capacitance as seen in Figure 3A, but the RC time constant τ is becoming larger for thicker transducing films than for the thinner transducing films. A larger RC time constant results in a longer required equilibration time to recover to the equilibrium state. Clearly, if the time required to reach equilibrium is longer for the thicker transducing films, the change in cumulated charge must also be more pronounced as the charge is integrated from the current over time. One therefore should observe a higher sensitivity for a concentration change with thicker transducing films but at the price of a longer recovery time (Figure 3B). The integration of the current expressed in eq. 6 predicts that the cumulated charge is linearly dependent on the ion activity change in the sample. Figure 3C shows calculated changes in sensitivity of the electrode responses with different capacitances of the transducing layer to changes in ion activity. A higher capacitance of the transducing layer results in more sensitive response towards changes in ion activity. Figures 3D-F show the predicted dependence of the current amplitude and integrated charge on the cell resistance for a given capacitance. Figure 3D displays how the transient current peaks upon changing the sample concentration, giving a decaying current transient with a time constant RC that is function of the capacitance of the transducing layer C_{cp} and the cell resistance R_{cell}. Figure 3E gives the cumulated charge integrated from the current over time for the concentration change, which is a function of the cell resistance at given capacitance. If one varies the cell resistance, the observed peak current amplitude decreases with increasing resistivity (Figure 3D) and the RC time constant τ is becoming larger for a more resistant transducing film but the overall cumulated charge (Figure 3F) is the same.

To test the theory and elucidate the role and the mechanism of the inner transducing layer at the electrode | membrane interface in constant potential coulometry, Prussian blue (PB) was chosen as an ideal model system. PB is a sodium-capacitor and is known for its high ion storage capacity and structural stability.[32-34] The general formula of PB is $Na_xFe[Fe(CN)_6]_y \bullet \square_{1-y} \bullet mH_2O$ ($0 < x < 2$, $y < 1$), where the square $\square$ expresses a $[Fe(CN)_6]$ vacancy taken up by coordinating water.[35] PB forms cubic crystals with few vacancies that can host sodium ions and may undergo a two-electron redox reaction as follows:[32]

$$Na_xFe^{III}Fe^{III}(CN)_6 \rightleftharpoons 2Na^+ + Na_{x-2}Fe^{II}Fe^{II}(CN)_6 + 2e^- \quad (7)$$

Figure S2A illustrates an initial system based on a pure PB capacitor without any overlaying ion-selective membrane with the proposed mechanism of sodium insertion or extraction into the PB crystal. A change in the ion activity in the bulk solution results in a potential change at the transducing layer | sample interface. Since the potential of the system is forced to stay constant, any incorporation of sodium ions into the crystal of Prussian blue will result in reduction of iron(III) to iron(II) to maintain electro-neutrality and a negative transient current will occur until a new equilibrium state is established. The transient current that results as a response to the activity change in the sample can be predicted and calculated from eq. 4. A very good correlation between the experimentally obtained reduction current (dots) and predicted trace derived from eq. 4 is shown in Figure 4. The observed transient reduction current is shown in Figure S3A and the cumulated charge passed through the PB modified electrode during a stepwise addition of 10^{-3} M to $10^{-0.6}$ M NaCl vs time is shown in Figure S3B.

To explore whether the mechanism would also be applicable in more complex systems, an ion-selective membrane was deposited on top of the Prussian blue layer. Unfortunately owing to significant solubility of Prussian blue in the polymeric membrane, as evidenced by a visible membrane color change from colorless to green, it was not possible to use PB as a transduction layer. Instead, the conducting polymer PEDOT doped with chloride ions was electropolymerized on the electrode substrate and used as inner transducing layer.

Two different configurations were explored here in detail, a membrane free electrode discussed earlier (Figure S2A) and

an anion-exchange membrane electrode backside contacted with PEDOT doped with chloride ions (Figure S2B).[36,37] All active components were freely dissolved in the hydrophobic polymeric matrix. The membrane was composed of ion exchanger TDMACl, NPOE as a polar plasticizer and poly(vinyl chloride). The anticipated sensing mechanisms of the ion-exchange process are shown in Figure 1. The anion-exchange membrane backside contacted with chloride doped PEDOT exhibits anion-exchange properties. As the potential of the system is again forced to remain constant, the potential change at the membrane | sample interface will cause a potential change at the membrane | conducting film interface upon a sample concentration change. For every dilution step, the potential at the membrane | sample interface increases, which means that part of $PEDOT^+(Cl^-)$ is reduced to $PEDOT^0$ and a negative transient current occurs. One assumes that the potential change in the film happens as a result of changing the ratio of $PEDOT^+(Cl^-)/PEDOT^0$ to compensate the potential difference at the membrane | sample interface and the transient current from the oxidation/reduction of $PEDOT^+(Cl^-)/PEDOT^0$ occurs until a new equilibrium state is reached.

The main interest of this work was to confirm whether the theoretical expectations agree quantitatively with the experimental results. To fulfill this aim, we first focused our attention to study the influence of the redox capacitance of the $PEDOT^+(Cl^-)/PEDOT^0$ solid contact on the equilibration time. The capacitance of the film is proportional to the polymerization charge and therefore also to the PEDOT film thickness.[27] Figure S4B shows a linear increase of the capacitance, calculated from the imaginary component of impedance at the lowest frequency (Figure S4A), with polymerization charge of PEDOT film (For more information about the calculation see Supporting Information). The goal was to keep the resistance of the cell R_{cell} constant while varying the capacitance of the intermediate transducing layer. If one keeps the membrane thickness constant, and so the cell resistance, and varies the capacitance of the conducting polymer, one may observe a variation in current decays with different RC time constants for different film thicknesses of the conducting polymer (see Figure 5). As expected, the thicker conducting film required more time to reach equilibrium state (Figure 5A - D) and as a result, the current peaks became broader with a higher resulting charge for an increasing redox capacitance of the conducting polymer transducer. Therefore, one needs to find a compromise situation between the peak height, response time and the total cumulated charge as a function of concentration change. The obtained results are in agreement with the theoretical expectations proposed here (see Figure 5). The integration of the current peaks observed for different concentration changes allows one to obtain information about the total cumulated charges transferred in the redox reaction. The linear dependence of the charge passed through the electrode as a function of logarithm of ion activity is shown in Figure S5 and agrees with eq 6.

Another important parameter that needs to be considered is the resistive overlaying ion-selective membrane and its influence on the cell resistance, the equilibration process and the response time. One may need additionally to consider mass transport across the membrane in relatively thick films (hundreds of μm), which is not considered in the simple theory above. From that point of view, thin membranes (hundreds of nm) may be advantageous as diffusional mass transport is rapid and the membrane resistance is also significantly lowered (Figure S6A). The membrane resistance can be also lowered by the addition of an inert lipophilic salt into the membrane (Figure S6B). The transient current peaks become sharper and narrower with thin films prepared by spin-coating and equilibrium is reached in a shorter time than for films prepared by conventional drop-casting (Figure 6). There is no significant difference between the cumulated charge for thin membranes prepared by spin-coating and for thick membranes prepared by drop-casting with less than 25 μL of membrane cocktail (Figure S6C). The cumulated charge is significantly lower for the film prepared by casting of 60 μL of membrane cocktail, most likely owing to insufficient time to reach equilibrium.

This coulometric readout method is potentially very attractive for applications where very small concentration changes should be monitored, such as personal health monitoring, environmental monitoring of pH and chloride in seawater or clinical analysis. To explore this, the sensitivity of this transduction method towards small concentration changes of primary ion was evaluated in preliminary work. The smallest concentration change performed was a 20 μM decrease in a 10 mM solution, a 0.2% change relative to the starting concentration was still easily measurable (the signal to noise ratio of 3.4 is useful for estimating the LOD, see Figure S7A). In direct potentiometry with ion-selective electrodes, the same concentration change gives a potential change of just 0.051 mV (Nernst equation), which is practically very challenging.

The method has been also tested in standard addition mode where successive amounts of a chloride standard were added to solution. The transient current (Figure 7A) monitored during the additions was converted to charge (Figure 7B) and plotted as a function of logarithm of chloride concentration. Figure 7C shows a linear dependence of the charge on the logarithmic concentration change in the sample. A comparison of the cumulated charge as a function of logarithmic chloride activity for drop casted and spin coated films is shown in Figures S8. The sensor response started to deviate from linear behavior for the lowest and highest concentrations owing to longer recovery times.

CONCLUSIONS

We explored constant potential coulometry as alternate readout for solid-contact ion-selective electrodes, with the detection of anions as a main focus. The experimental data were accompanied with a simplified theory that adequately explained the results. Prussian blue was used as a simple sodium capacitor to demonstrate the role of the transduction layer as capacitor, while PEDOT(Cl) was used as transduction layer in the anion-selective electrode studies. We demonstrated how the membrane resistance, thickness of the conducting polymer and the ion-selective membrane influence the transient current, the response time and total cumulated charge. The method exhibits attractive sensitivity, stability and reproducibility with a relatively quick response time to concentration changes of anions at high concentrations. A remarkable improvement in shortening the response time was achieved with very thin ion-selective membranes spin-coated on the conducting polymer support. The utility of the sensor was illustrated by detecting very small concentration changes down to 0.2%. This approach is expected to find future applications for assessing very small concentration changes in a range of important applications, including seawater monitoring.

ASSOCIATED CONTENT

Supporting Information

Additional data such as data presentation, experimental current-time and charge-time curves for Prussian blue based electrodes,

electrochemical impedance spectra recorder for different redox capacity, different membrane thickness and membrane composition, standard addition mode for spin coat and drop cast film, reversibility of the sensor and determination of LOD.

The Supporting Information is available free of charge on the ACS Publications website.

AUTHOR INFORMATION

Corresponding Authors

* eric.bakker@unige.ch, johan.bobacka@abo.fi

ACKNOWLEDGMENT

The authors thank the Swiss National Foundation, the University of Geneva, the Johan Gadolin Scholarship Program and Åbo Akademi University for supporting this research.

REFERENCES

(1) Bakker, E.; Diamond, D.; Lewenstam, A.; Pretsch, E. Ion Sensors: Current Limits and New Trends. *Anal. Chim. Acta* **1999**, *393*, 11-18.
(2) Bakker, E.; Pretsch, E. Potentiometry at Trace Levels. *Trends Anal. Chem.* **2001**, *20*, 11-19.
(3) Konopka, A.; Sokalski, T.; Michalska, A.; Lewenstam, A.; Maj-Zurawska, M. Factors Affecting the Potentiometric Response of All-Solid-State Solvent Polymeric Membrane Calcium-Selective Electrode for Low-Level Measurements. *Anal. Chem.* **2004**, *76*, 6410-6418.
(4) Lewenstam, A.; Maj-Zurawska, M.; Hulanicki, A. Application of Ion-Selective Electrodes in Clinical Analysis. *Electroanalysis* **1991**, *3*, 727-734.
(5) Xie, X.; Zhai, J.; Bakker, E. Potentiometric Response from Ion-Selective Nanospheres with Voltage-Sensitive Dyes. *J. Am. Chem. Sci.* **2014**, *136*, 16465-16468.
(6) Murkovic, I.; Lobnik, A.; Mohr, G. J.; Wolfbeis, O. S. Fluorescent Potential-Sensitive Dyes for Use in Solid State Sensors for Potassium Ion. *Anal. Chim. Acta* **1996**, *334*, 125-132.
(7) Wolfbeis, O. S. Fluorescence-Based Ion Sensing Using Potential-Sensitive Dyes. *Sens. Actuators B Chem.* **1995**, *29*, 140-147.
(8) Stashkova, A. E.; Peshkova, M. A.; Mikhelson, K. N. Single-Ion Activity: Optical Sensing vs. Electrochemical Sensing. *Sens Actuators B Chem.* **2015**, *207*, 346-350.
(9) Crespo, G. A.; Mistlberger, G.; Bakker, E. Electrogenerated Chemiluminescence for Potentiometric Sensors. *J. Am. Chem. Sci.* **2012**, *134*, 205-207.
(10) Zhang, X.; Han, Y.; Li, J.; Zhang, L.; Jia, X.; Wang, E. Portable, Universal, and Visual Ion Sensing Platform Based on the Light Emitting Diode-Based Self-Referencing-Ion Selective Field-Effect Transistor. *Anal. Chem.* **2014**, *86*, 1380-1384.
(11) Hupa, E.; Vanamo, U.; Bobacka, J. Novel ion-to-Electron Transduction Principle for Solid-Contact ISEs. *Electroanalysis* **2015**, *27*, 591-594.
(12) Bobacka, J. Potential Stability of All-Solid-State Ion-Selective Electrodes Using Conducting Polymers as Ion-to-Electron Transducers. *Anal. Chem.* **1999**, *71*, 4932-4937.
(13) Rius-Ruiz, F. X.; Bejarano-Nosas, D.; Blondeau, P.; Riu, J.; Rius, F. X. Disposable Planar Reference Electrode Based on Carbon Nanotubes and Polyacrylate Membrane. *Anal. Chem.* **2011**, *83*, 5783-5788.
(14) Fibbioli, M.; Morf, W. E.; Badertscher, M.; De Rooij, N. F.; Pretsch, E. Potential Drifts of Solid−Contacted Ion−Selective Electrodes Due to Zero−Current Ion Fluxes Through the Sensor Membrane. *Electroanalysis* **2000**, *12*, 1286-1292.
(15) Fouskaki, M.; Chaniotakis, N. Fullerene-Based Electrochemical Buffer Layer for Ion-Selective Electrodes. *Analyst* **2008**, *133*, 1072-1075.
(16) Lai, C. Z.; Fierke, M. A.; Stein, A.; Buhlmann, P. Ion-Selective Electrodes with Three-Dimensionally Ordered Macroporous Carbon as the Solid Contact. *Anal. Chem.* **2007**, *79*, 4621-4626.
(17) Li, F.; Ye, J.; Zhou, M.; Gan, S.; Zhang, Q.; Han, D.; Niu, L. All-Solid-State Potassium-Selective Electrode Using Graphene as the Solid Contact. *Analyst* **2012**, *137*, 618-623.
(18) Ping, J.; Wang, Y.; Ying, Y.; Wu, J. Application of Electrochemically Reduced Graphene Oxide on Screen-Printed Ion-Selective Electrode. *Anal. Chem.* **2012**, *84*, 3473-3479.
(19) Jaworska, E.; Wojcik, M.; Kisiel, A.; Miesczkowski, J.; Michalska, A. Application of Electrochemically Reduced Graphene Oxide on Screen-Printed Ion-Selective Electrode. *Talanta* **2011**, *85*, 1986-1989.
(20) Grygolowicz-Pawlak, E.; Plachecka, K.; Brzozka, Z.; Malinowska, E. Further Studies on the Role of Redox-active Monolayer as Intermediate Phase of Solid-State Sensors. *Sens. Actuators B Chem.* **2007**, *123*, 480-487.
(21) Veder, J. P.; De Marco, R.; Patel, K.; Si, P. C.; Grygolowicz-Pawlak, E.; James, M.; Alam, M. T.; Sohail, M.; Lee, J.; Pretsch, E.; Bakker, E. Evidence for a Surface Confined Ion-to-Electron Transduction Reaction in Solid-Contact Ion-Selective Electrodes Based on Poly(3-octylthiophene). *Anal. Chem.* **2013**, *85*, 10495-10502.
(22) Bobacka, J. Conducting Polymer-Based Solid-State Ion-Selective Electrodes. *Electroanalysis* **2006**, *18*, 7-18.
(23) Michalska, A. All-Solid-State Ion Selective and All-Solid-State Reference Electrodes. *Electroanalysis* **2012**, *24*, 1253-1265.
(24) Bobacka, J.; Ivaska, A.; Lewenstam, A. Potentiometric Ion Sensors. *Chem. Rev.* **2008**, *108*, 329-351.
(25) Vanamo, U.; Hupa, E.; Yrjana, V.; Bobacka, J. New Signal Readout Principle for Solid-Contact Ion-Selective Electrodes. *Anal. Chem.* **2016**, *88*, 4369-4374.
(26) Han, T.; Vanamo, U.; Bobacka, J. Influence of Electrode Geometry on the Response of Solid-Contact Ion-Selective Electrodes when Utilizing a New Coulometric Signal Readout Method. *ChemElectroChem.* **2016**, *3*, 2071-2077.
(27) Bobacka, J.; Lewenstam, A.; Ivaska, A. Electrochemical Impedance Spectroscopy of Oxidized Poly(3,4-ethylenedioxythiophene) Film Electrodes in Aqueous Solutions. *J. Electroanal. Chem.* **2000**, *489*, 17-27.
(28) Liu, X.; Nan, Z.; Qiu, Y.; Zheng, L.; Lu, X. Hydrophobic Ionic Liquid Immoblizing Cholesterol Oxidase on the Electrodeposited Prussian Blue on Glassy Carbon Electrode for Detection of Cholesterol. *Electrochim. Acta* **2013**, *90*, 203-209.
(29) Cuartero, M.; Crespo, G. A.; Bakker, E. Polyurethane Ionophore-Based Thin Layer Membranes for Voltammetric Ion Activity Sensing. *Anal. Chem.* **2016**, *88*, 5649-5654.
(30) Crespo, G. A.; Cuartero, M.; Bakker, E. Thin Layer Ionophore-Based Membrane for Multianalyte Ion Activity Detection. *Anal. Chem.* **2015**, *87*, 7729-7737.
(31) Si, P.; Bakker, E. Thin Layer Electrochemical Extraction of Non-redoxactive Cations with an Anion-Exchanging Conducting Polymer Overlaid with a Selective Membrane. *Chem. Commun.* **2009**, 5260-5262.
(32) Zhou, L.; Yang, Z.; Li, C.; Chen, B.; Wang, Y.; Fu, L.; Zhu, Y.; Liu, X.; Wu, Y. Prussian Blue as Positive Electrode Material for Aqueous Sodium-Ion Capacitor with Excellent Performance. *RSC Advances* **2016**, *6*, 109340-109345.

(33) Wang, L.; Lu, Y.; Liu, J.; Xu, M.; Cheng, J.; Zhang, D.; Goodenough, J. B. A Superior Low-Cost Cathode for a Na-Ion Battery. *Angew. Chem. Int. Ed.* **2013**, *52*, 1964-1967.
(34) Matsuda, T.; Takachi, M.; Moritomo, Y. A Sodium Manganese Ferrocyanide Thin Film for Na-Ion Batteries. *Chem. Commun.* **2013**, *49*, 2750-2752.
(35) Asakura, D.; Okubo, M.; Mizuno, Y.; Kudo, T.; Zhou, H.; Ikedo, K.; Mizokawa, T.; Okazawa, A.; Kojima, N. Fabrication of a Cyanide-Bridged Coordination Polymer Electrode for Enhanced Electrochemical Ion Storage Ability. *J. Phys. Chem. C* **2012**, *116*, 8364-8369.
(36) Bratov, A.; Abramova, N.; Dominguez, C. Investigation of Chloride Sensitive ISFETs with Different Membrane Compositions Suitable for Medical Applications. *Anal. Chim. Acta* **2004**, *514*, 99-106.
(37) Rothmaier, M.; Simon, W. Chloride-Selective Electrodes Based on Mercury Organic Compounds as Neutral Carriers. *Anal. Chim. Acta* **1993**, *271*, 135-141.

Table 1. Compositions of the investigated membranes (in mg).

	M1	M2	M3	M4	M5	M6
ETH 9009	-	2	2	2	2	2
TDMACl	30	0.3	0.03	0.03	0.03	0.03
DOS	-	64.7	64.97	58.6	55.3	64.6
NPOE	102	-	-	-		-
PVC	68	33	33	29.3	27.7	32.3
ETH 500	-	-	-	10	15	1

FIGURES

Figure 1 Schematic illustration of the working transduction mechanism for a simple capacitor covered with ion-selective membrane. Any change in the ion activity in a bulk solution (s) results in a potential change at the sample | transducing layer. Since the system is held at a constant potential, any change in ion activity will result in changing of the ratio of oxidized and reduced form of the transducing layer (TL) and the transient current will occur until the new equilibrium state is reached.

Figure 2 Schematic illustration of current response of the system described according to Equation 4(A) with corresponding cumulated charge (B) as a function of capacitance and cell resistance. Parameters used: R = 100 kΩ, C = 0.1 mF.

Figure 3 Comparison of the current-time curves (A) of capacitor with different capacitances with corresponding cumulated charge (B) and its logarithmic dependence of the charge on the ion activity (C). Parameters used: R = 175 kΩ, C = 0.026 – 0.26 mF. Comparison of the current-time curves (D) of capacitor with different cell resistance with corresponding cumulated charge (E) and its logarithmic dependence of the charge on the ion activity (F). Parameters used: R = 50 - 1000 kΩ, C = 0.52 mF.

Figure 4 A) Comparison of the experimentally obtained current-time curves for Prussian Blue modified electrodes (dots) with theoretical expectations (solid line). B) Cumulated charge Q vs logarithmic sodium activity for the Prussian blue solid contact electrode measured by consecutive additions. Parameters used: R = 1.275 kΩ, C = 0.32 mF obtained from the EIS experiments.

Figure 5 Enlargement of the chronoamperograms recorded for anion-sensitive SC-ISEs (25 µL of M1) with different redox capacity of PEDOT(Cl) solid contacts experimentally obtained (dots) fitted with theory (solid line). Parameters used: R = 181 kΩ (obtained from the EIS experiments shown in Figure S6), $C_{1\ mC}$ = 0.026 mF, $C_{2\ mC}$ = 0.053 mF, $C_{4\ mC}$ = 0.099 mF, $C_{10\ mC}$ = 0.25 mF (estimated capacitance for different PEDOT film thickness was obtained from the EIS experiments shown in Figure S4).

Figure 6 Comparison of chronoamperograms experimentally obtained for anion-sensitive SC-ISEs with 10 mC of PEDOT(Cl) solid contacts covered with different membrane thicknesses (M1).

Figure 7 Experimental current-time (A) and charge-time (B) curves for standard addition for drop casted anion-selective membrane (M1). C) Cumulated charge Q vs logarithm of the activity for chloride-sensitive SC-ISE (M1) with 10 mC of PEDOT(Cl) solid contacts measured in standard addition mode for drop casted film (M1).

FOR TOC ONLY

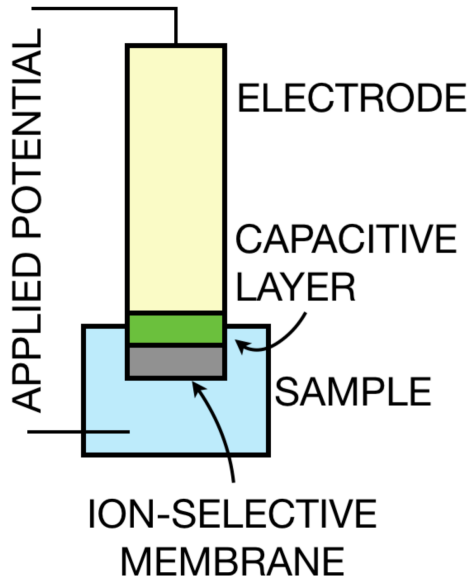
APPLIED POTENTIAL
ELECTRODE
CAPACITIVE
LAYER
SAMPLE
ION-SELECTIVE
MEMBRANE

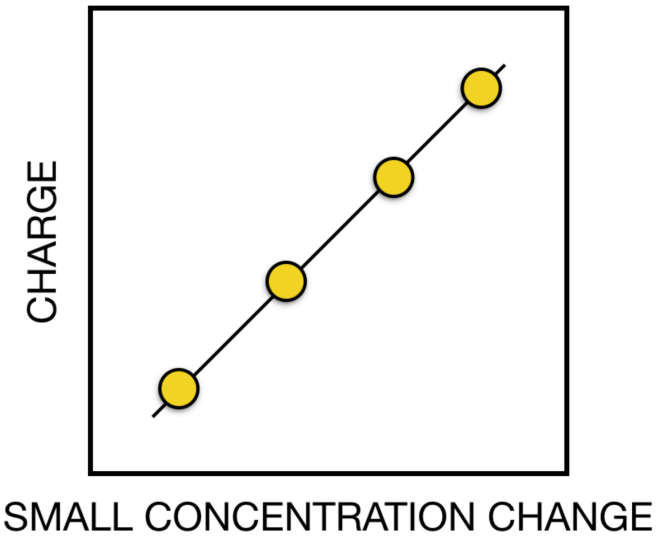
CHARGE
SMALL CONCENTRATION CHANGE

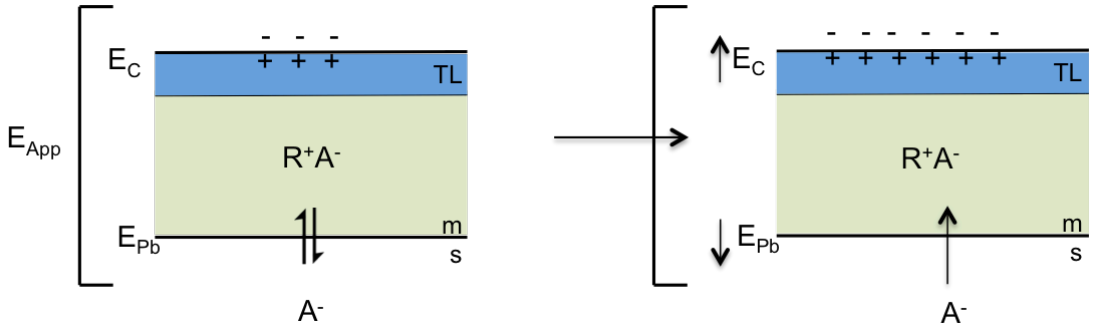

Figure 1

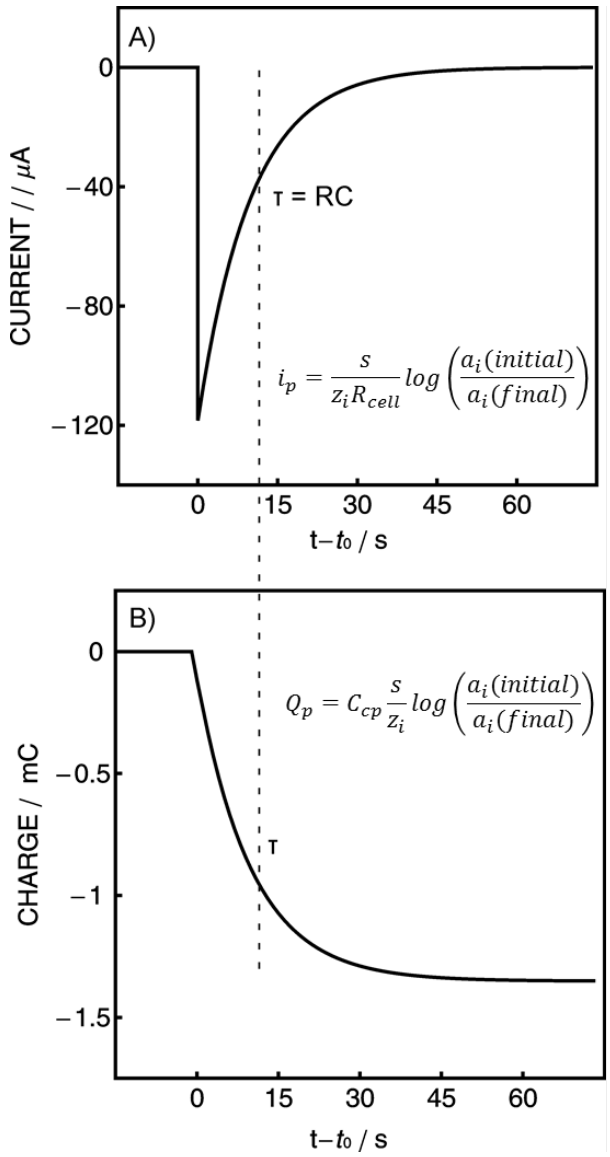
A)
0
−40
−80
−120
CURRENT / / μA
τ = RC
$i_p = \frac{s}{z_i R_{cell}} log\left(\frac{a_i(initial)}{a_i(final)}\right)$
0
15
30
45
60
t−t₀ / s
B)
0
−0.5
−1
−1.5
CHARGE / mC
τ
$Q_p = C_{cp}\frac{s}{z_i} log\left(\frac{a_i(initial)}{a_i(final)}\right)$
0
15
30
45
60
t−t₀ / s

Figure 2

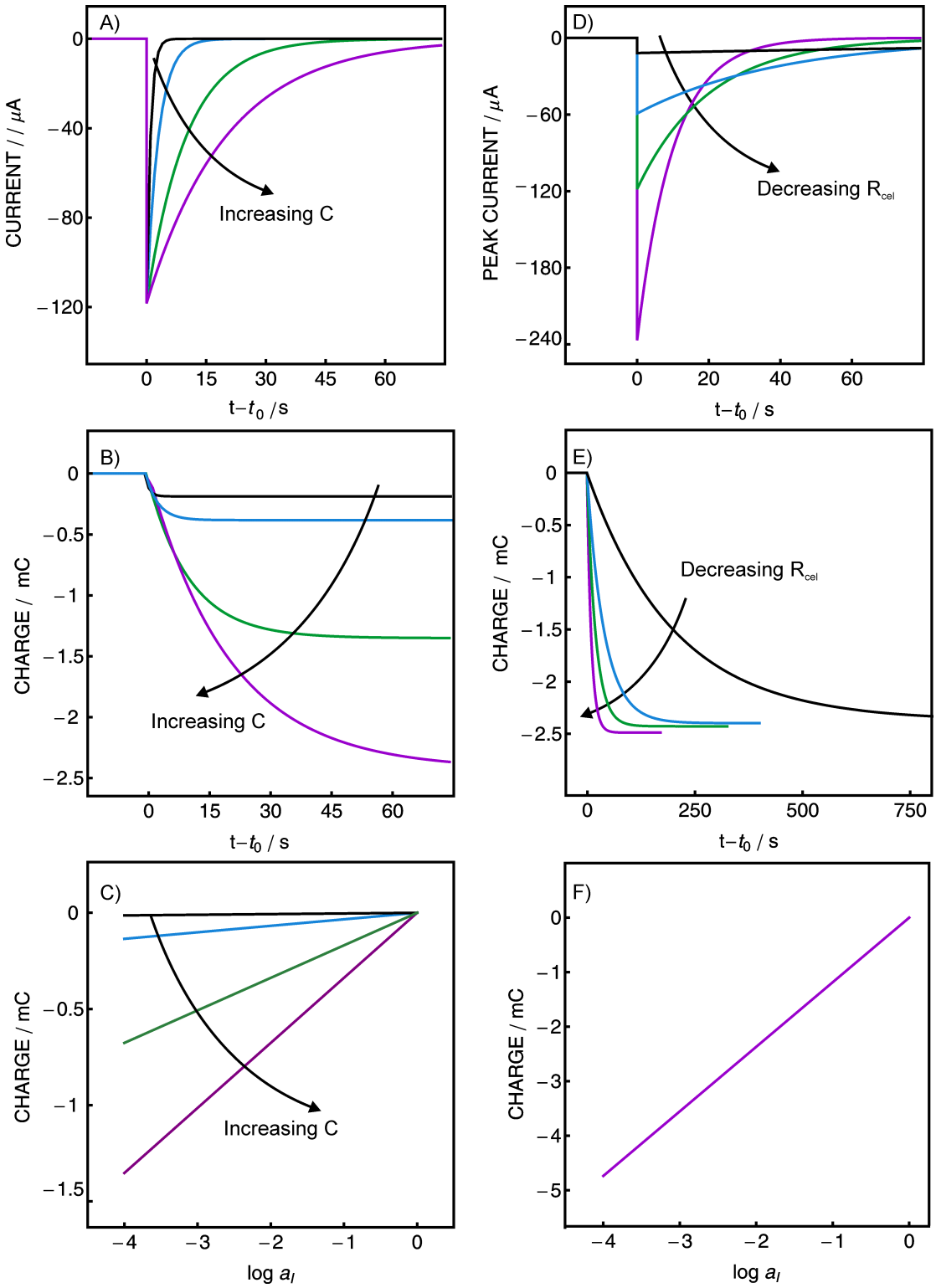
A)
CURRENT / / μA
0
−40
−80
−120
0
15
30
45
60
t−t0 /s
Increasing C
D)
PEAK CURRENT / μA
0
−60
−120
−180
−240
0
20
40
60
t−t0 / s
Decreasing Rcel
B)
CHARGE / mC
0
−0.5
−1
−1.5
−2
−2.5
0
15
30
45
60
t−t0 / s
Increasing C
E)
CHARGE / mC
0
−0.5
−1
−1.5
−2
−2.5
0
250
500
750
t−t0 / s
Decreasing Rcel
C)
CHARGE / mC
0
−0.5
−1
−1.5
−4
−3
−2
−1
0
log aI
Increasing C
F)
CHARGE / mC
0
−1
−2
−3
−4
−5
−4
−3
−2
−1
0
log aI

Figure 3

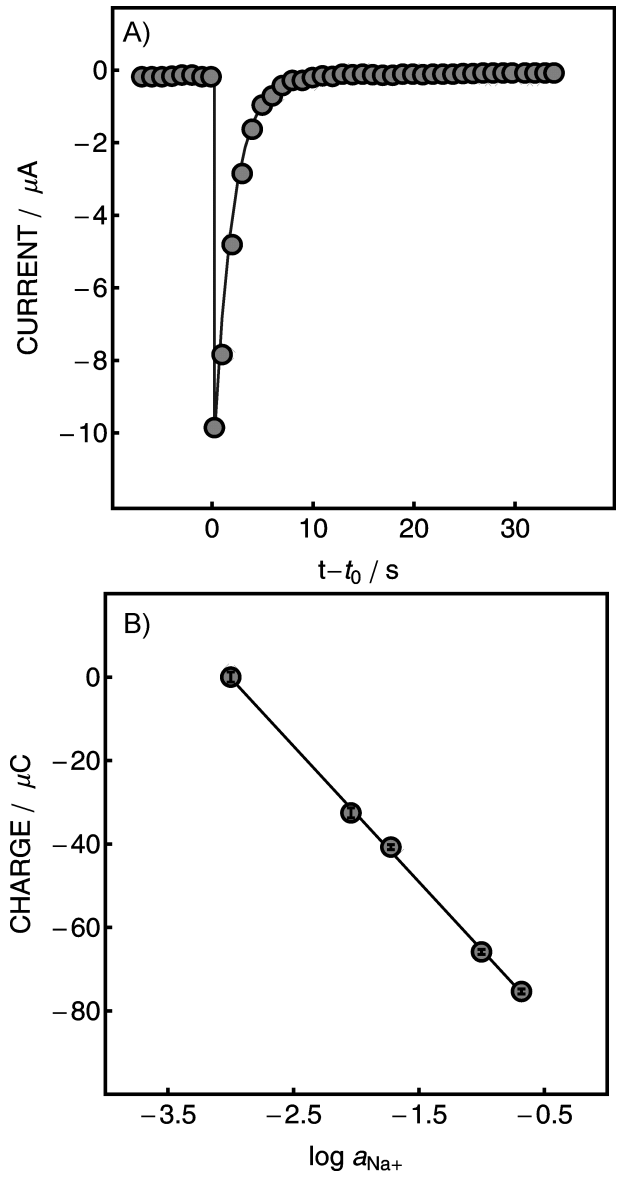
A)
0
−2
−4
−6
−8
−10
CURRENT / μA
0
10
20
30
t−t0 / s
B)
0
−20
−40
−60
−80
CHARGE / μC
−3.5
−2.5
−1.5
−0.5
log aNa+

Figure 4

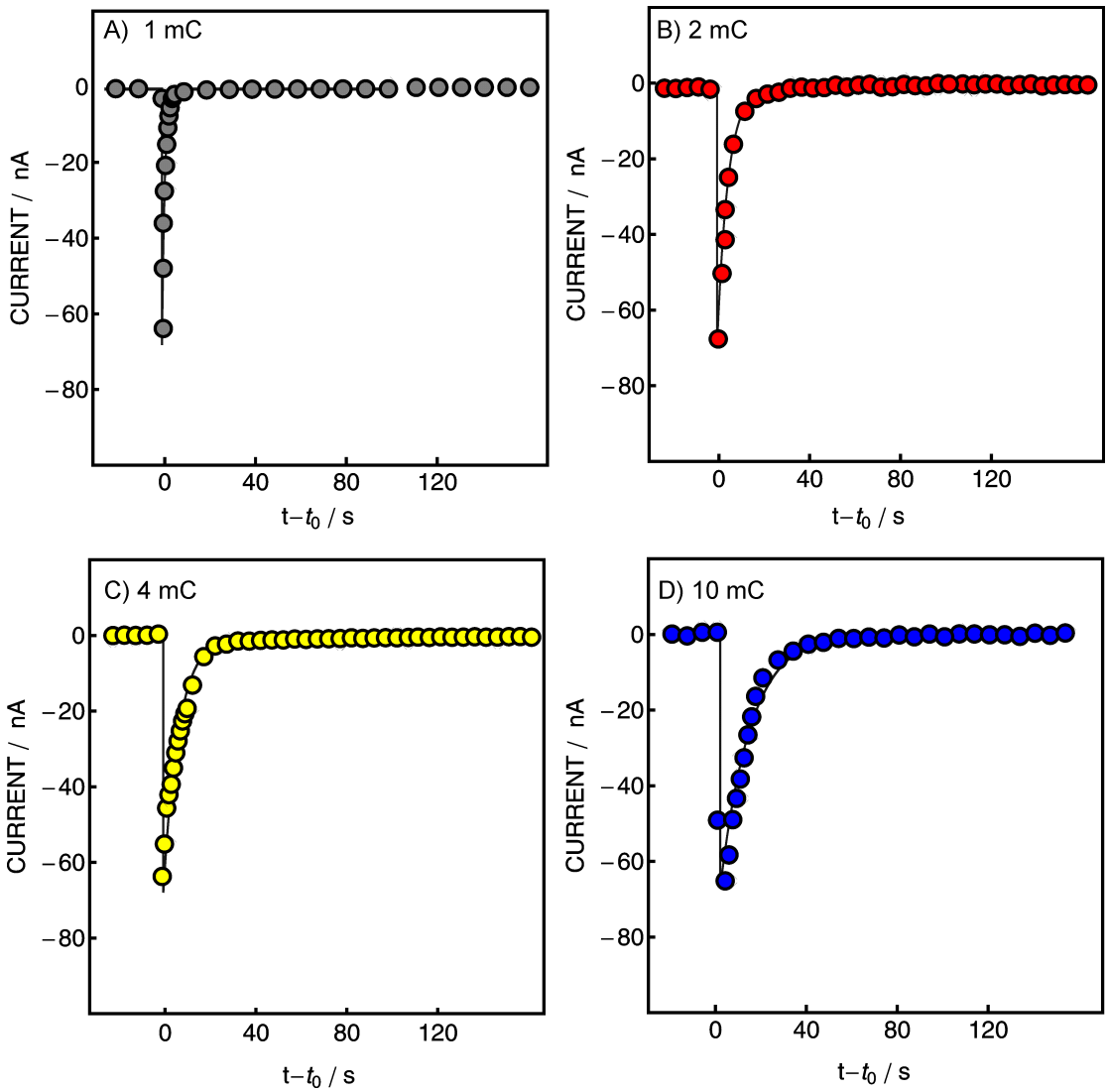

Figure 5

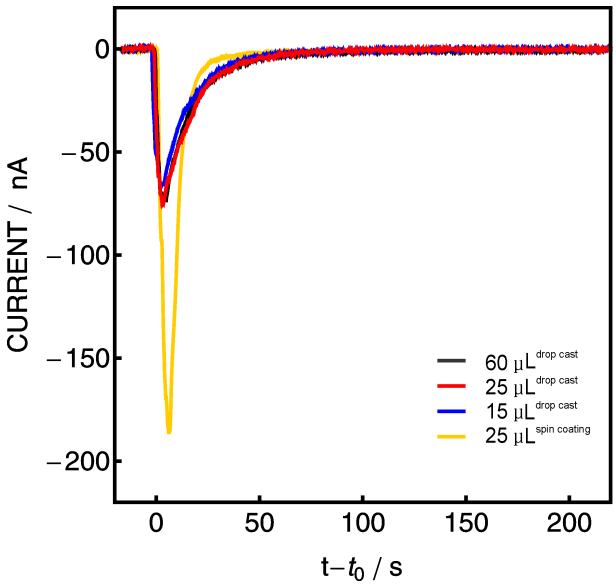
0
−50
−100
−150
−200
CURRENT / nA
0
50
100
150
200
t−t0 / s
60 µL drop cast
25 µL drop cast
15 µL drop cast
25 µL spin coating

Figure 6

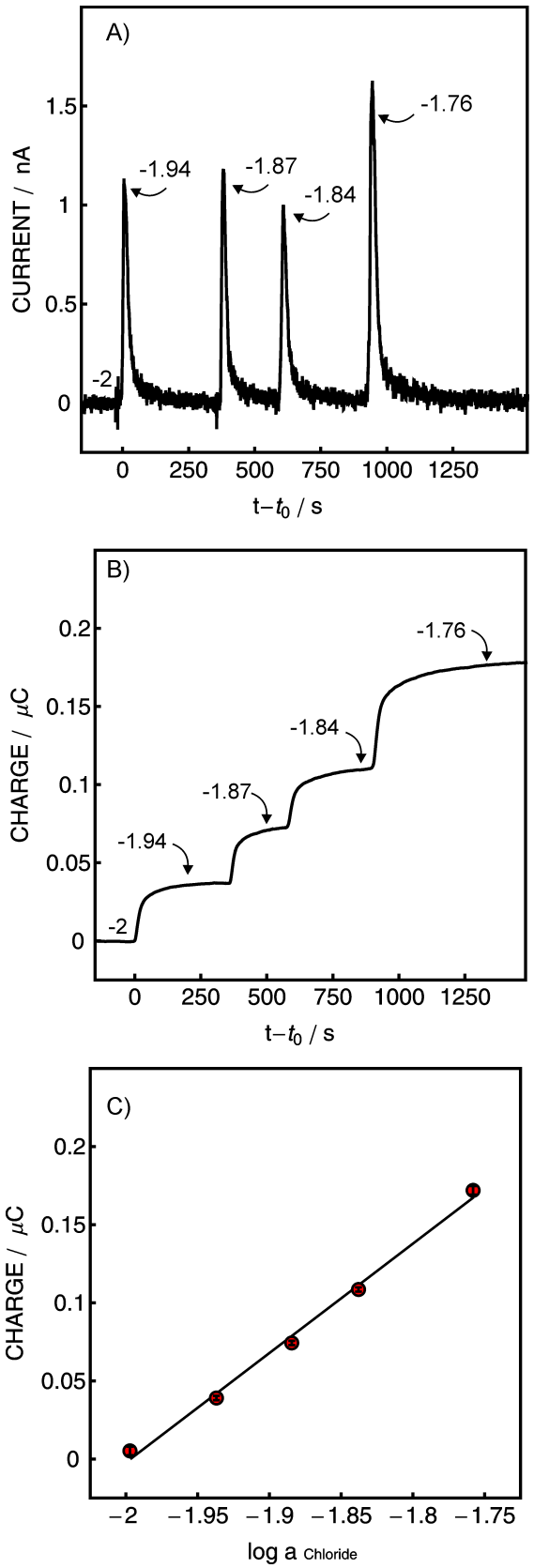
A)
CURRENT / nA
1.5
1
0.5
0
-2
-1.94
-1.87
-1.84
-1.76
0
250
500
750
1000
1250
t–t_0 / s
B)
CHARGE / μC
0.2
0.15
0.1
0.05
0
-2
-1.94
-1.87
-1.84
-1.76
0
250
500
750
1000
1250
t–t_0 / s
C)
CHARGE / μC
0.2
0.15
0.1
0.05
0
–2
–1.95
–1.9
–1.85
–1.8
–1.75
log a Chloride

Figure 7

Supporting Information for

Capacitive Model for Coulometric Readout of Ion-Selective Electrodes

Zdeňka Jarolímová,[a] Tingting Han,[b] Ulriika Mattinen,[b] Johan Bobacka,[b] and Eric Bakker [a]

[a] Department of Inorganic and Analytical Chemistry, University of Geneva, Quai Ernest Ansermet 30, 1211 Geneva 4 (Switzerland)
e-mail: eric.bakker@unige.ch
[b] Johan Gadolin Process Chemistry Centre, Laboratory of Analytical Chemistry, Åbo Akademi University
Biskopsgatan 8, FI-20500 Turku-Åbo (Finland)
e-mail: johan.bobacka@abo.fi

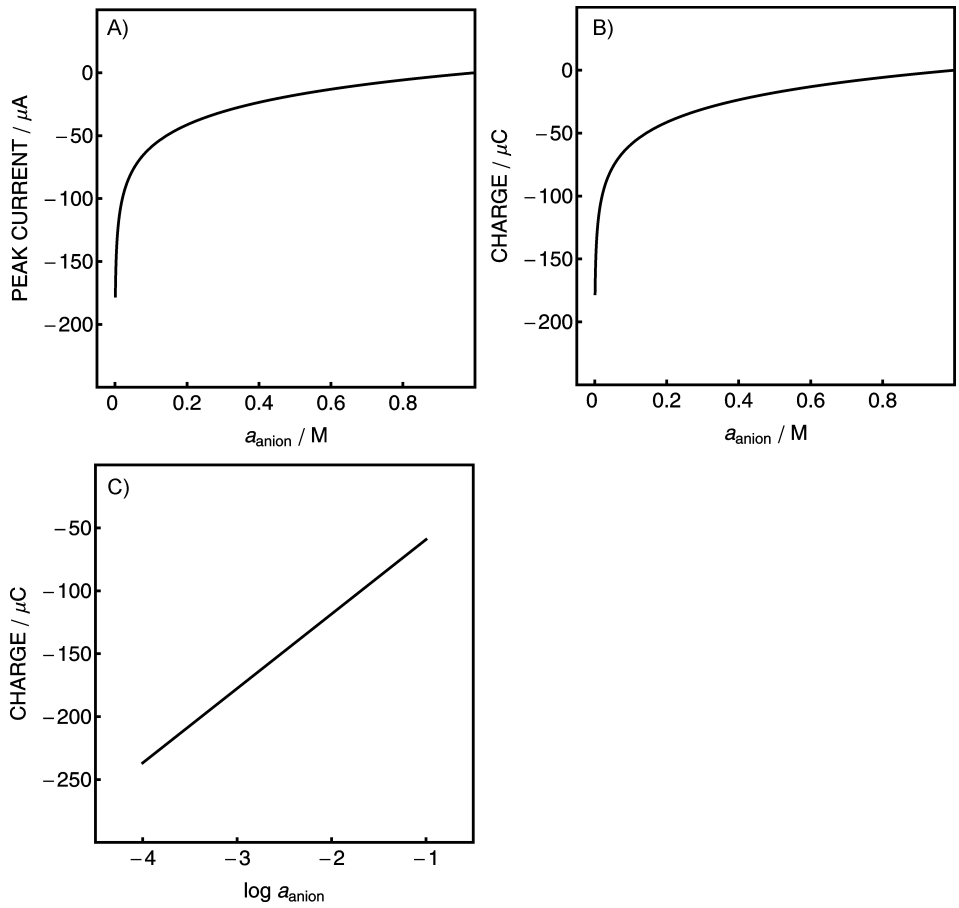

Figure S1 Data presentation: A) Calculated resulting transient current as a function of ion activity according to Equation 4. Parameters used: R = 1 kΩ, C = 1 mF. The current response is not linear in a wider range and the values depends on the resistance, therefore it is not recommended to plot peak current as a function of activity. B) Calculated resulting charge response of the system as a function of ion activity according to Equation 6. Parameters used: R = 1 kΩ. The charge is not linear and the values depend linearly on the capacitance, therefore it is not recommended to plot charge as a function of activity. C) Calculated charge response as a function of logarithmic ion activity according to Equation 6. Parameters used: C = 1 mF. The obtained charge response as a function of logarithmic ion activity is linear and is the recommended way to represent the data.

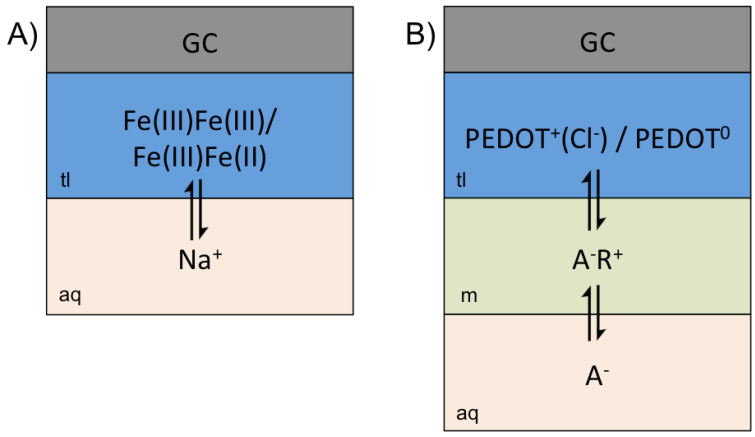

Figure S2 A) Schematic illustration of the working mechanism of the Prussian blue transducing layer (tl) as a simple sodium capacitor (A) and the ion-selective membrane (m) deposited on the conducting polymer tl (B). Any change in the ion activity in a bulk solution (aq) results in a potential change at the aq | tl (A) and aq | m (B) interfaces. Since the system is held at a constant potential, any change in ion activity will result in changing of the ratio of oxidized and reduced form of the transducing layer and the transient current will occur until the new equilibrium state is reached. In the solid-state membrane configuration, the membrane contains only ion-exchanger TDMACl (R^+Cl^-).

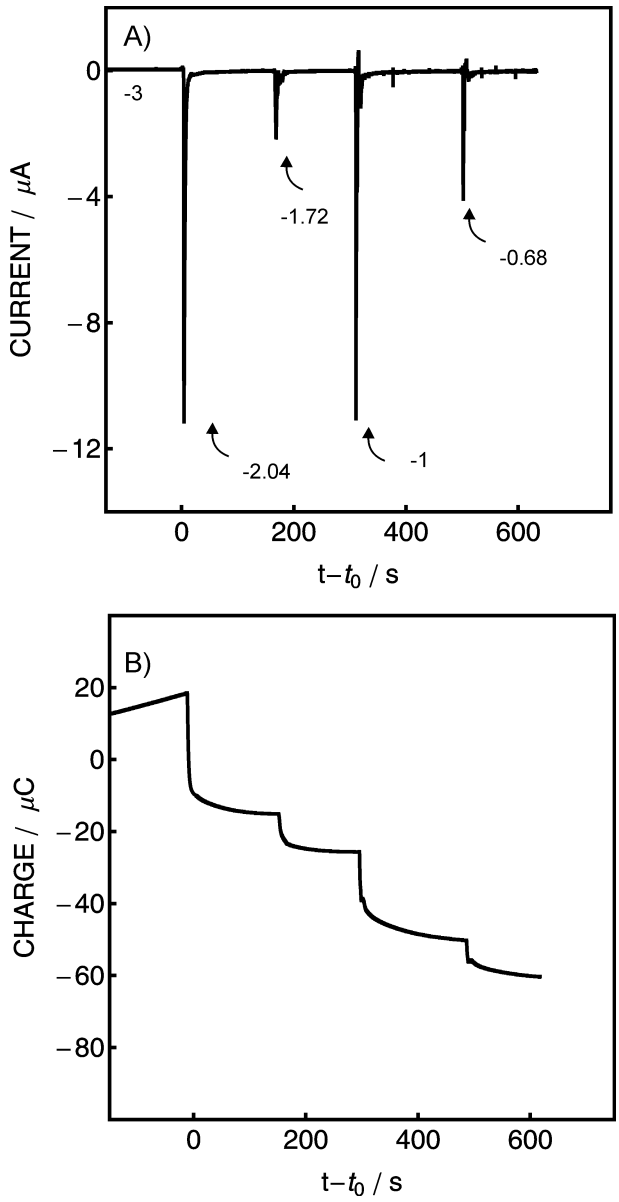

Figure S3 A) Experimentally obtained current-time curves recorded for Prussian blue based electrode to the successive addition of sodium chloride. Values shown are logarithmic sodium concentrations. B) Corresponding experimental charge-time curves recorded for Prussian blue based electrode to the successive addition of sodium chloride.

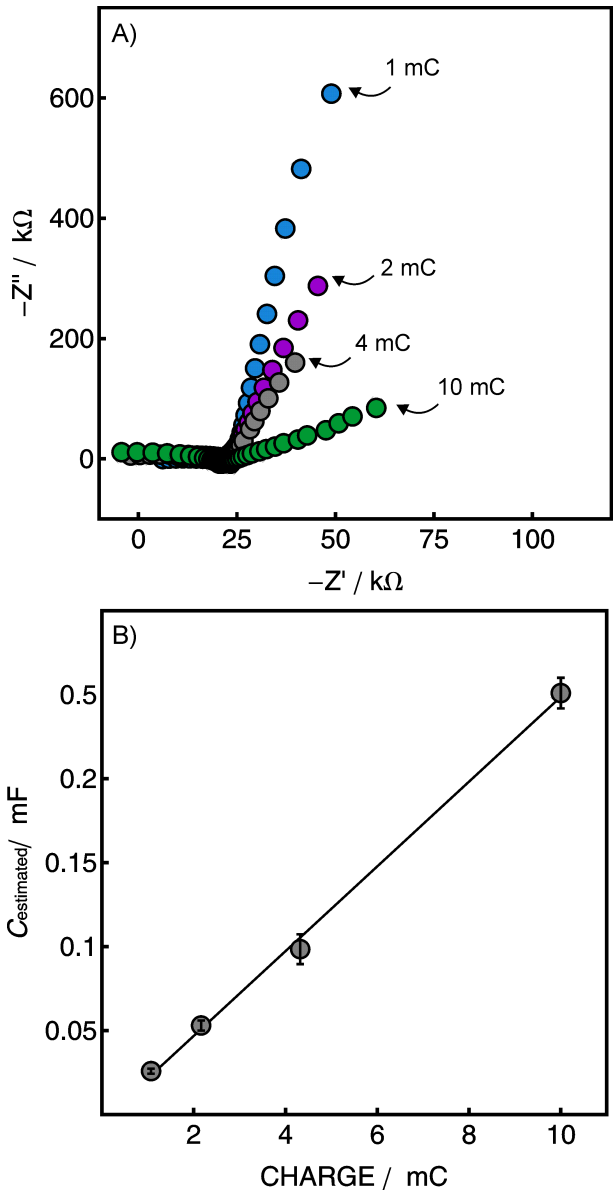

Figure S4 Comparison of impedance plots for different polymerization charge of PEDOT(Cl) covered with an anion-sensitive membrane electrode (25 µL spin-coated M1) in 0.01 M KCl solution (A). Observed capacitance as a function of polymerization charge for PEDOT(Cl) covered with an anion-sensitive membrane electrode (25 µL spin-coated M1) in 0.01 M KCl solution (B).

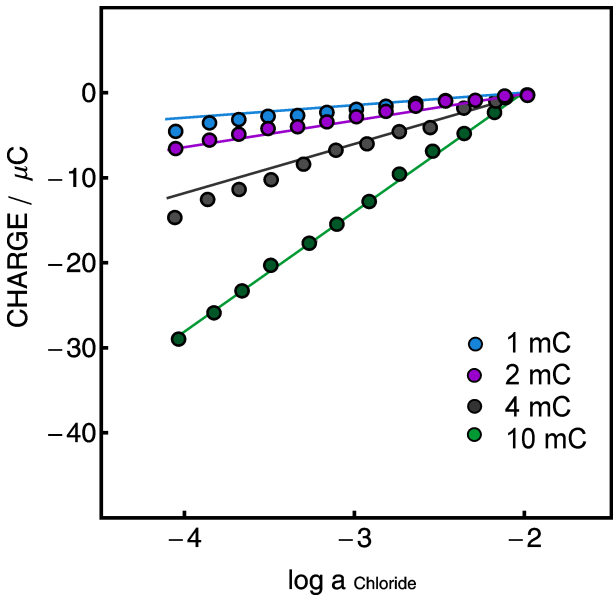

Figure S5 Experimental cumulative charge with altering ion concentration. Comparison of cumulated charge Q vs logarithm of the activity for an anion-sensitive SC-ISE (25 µL of M1) with different redox capacity of PEDOT(Cl) solid contacts. The starting solution of 10^{-2} M KCl was gradually diluted to 10^{-4} M. Experimentally obtained results (dots) were compared to the theoretical expectations (solid lines) calculated according to eq. 6. Parameters used: R = 181 kΩ (obtained from the EIS experiments shown in Figure S6), $C_{1\,mC}$ = 0.026 mF, $C_{2\,mC}$ = 0.053 mF, $C_{4\,mC}$ = 0.099 mF, $C_{10\,mC}$ = 0.25 mF (estimated capacitance for different PEDOT film thickness was obtained from the EIS experiments shown in Figure S4).

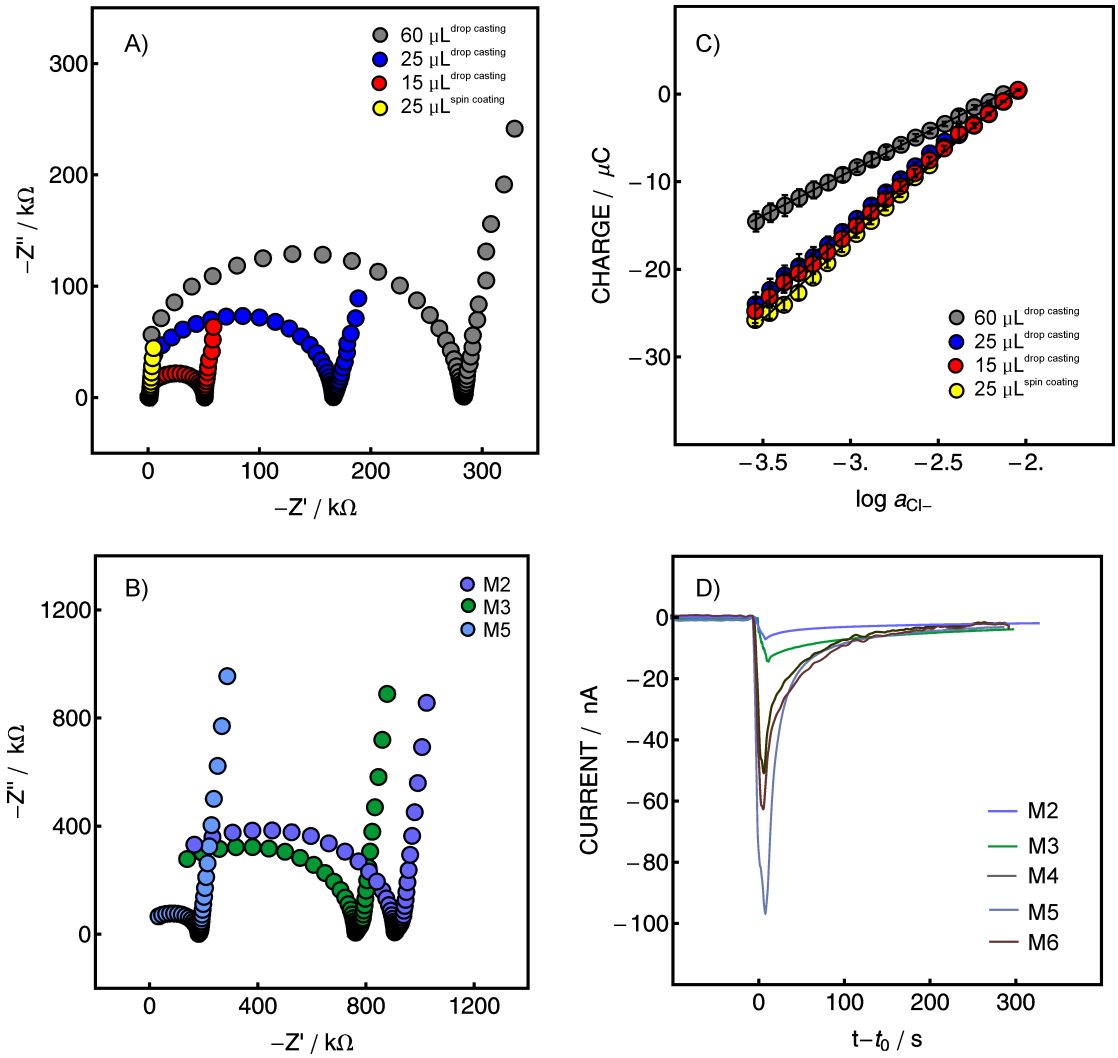

Figure S6 Electrochemical impedance spectra recorded for A) different thickness of the ion-exchange membrane and for B) different membrane compositions. C) Comparison of cumulated charge Q vs logarithm of the activity for an anion-sensitive SC-ISE (M1) with 10 mC of PEDOT(Cl) solid contacts covered with different membrane thickness (M1). The starting solution of 10^{-2} M KCl was gradually diluted to 10^{-4} M. D) Experimental current-time curves for anion-selective SC-ISEs of different resistivity.

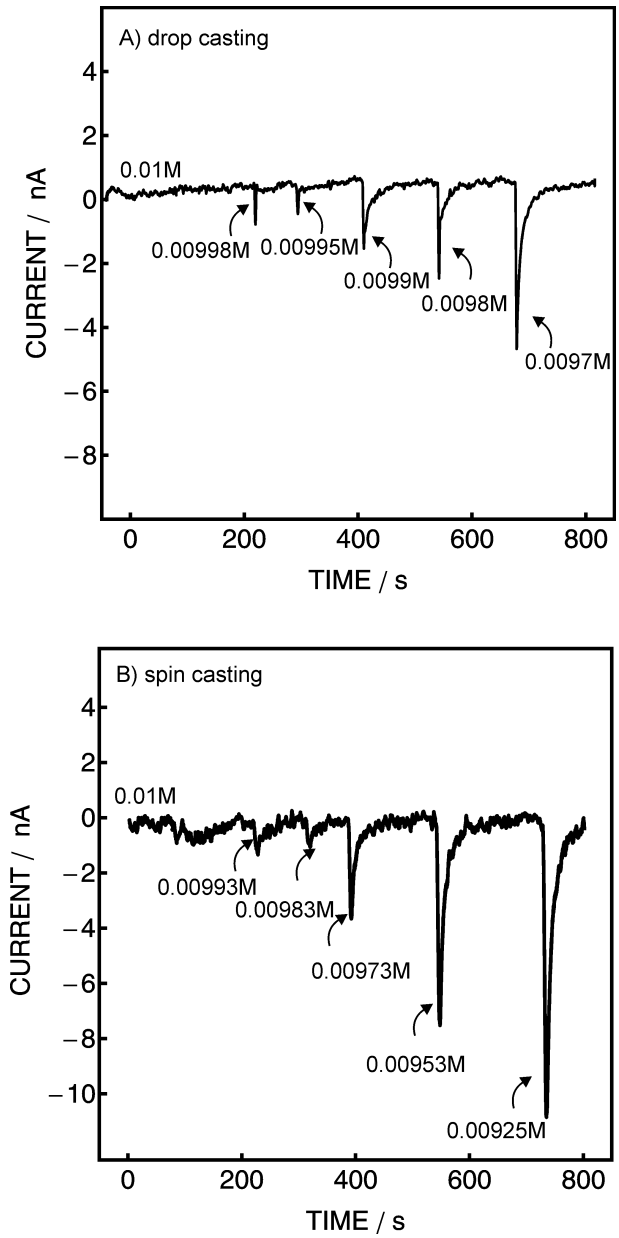

Figure S7 Limit of detection of 10 mC PEDOT(Cl) modified SC-ISE covered with drop cast (60 µm) (A) and spin coated (200 nm) (B) membrane films (M1). Values shown are logarithmic chloride concentrations. S/N is 3.43 for 20 µM addition to a 10 mM solution for a drop cast film and 3.18 for 70 µM addition to a 10 mM solution for spin coated film.

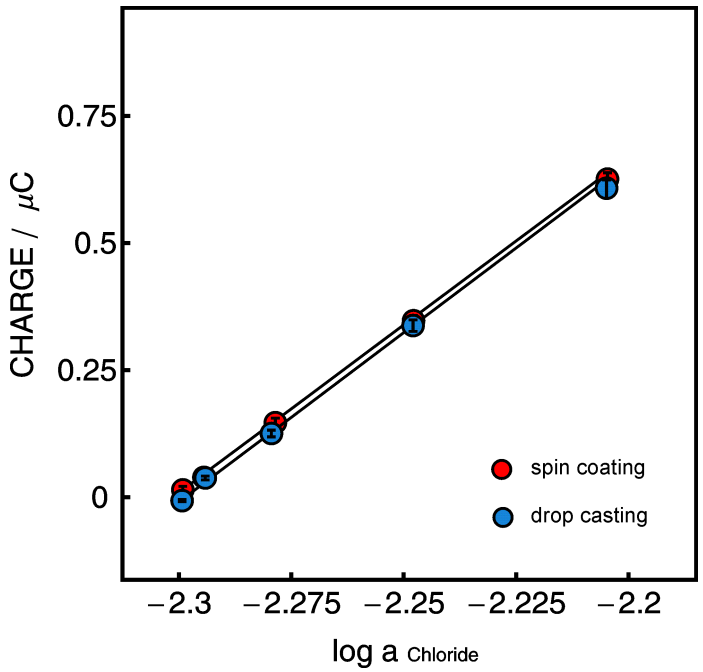

Figure S8 Cumulated charge Q vs logarithm of the chloride activity for an anion-sensitive SC-ISE (M1) with 10 mC of PEDOT(Cl) solid contacts for spin coated and drop cast films (M1) measured in addition mode.

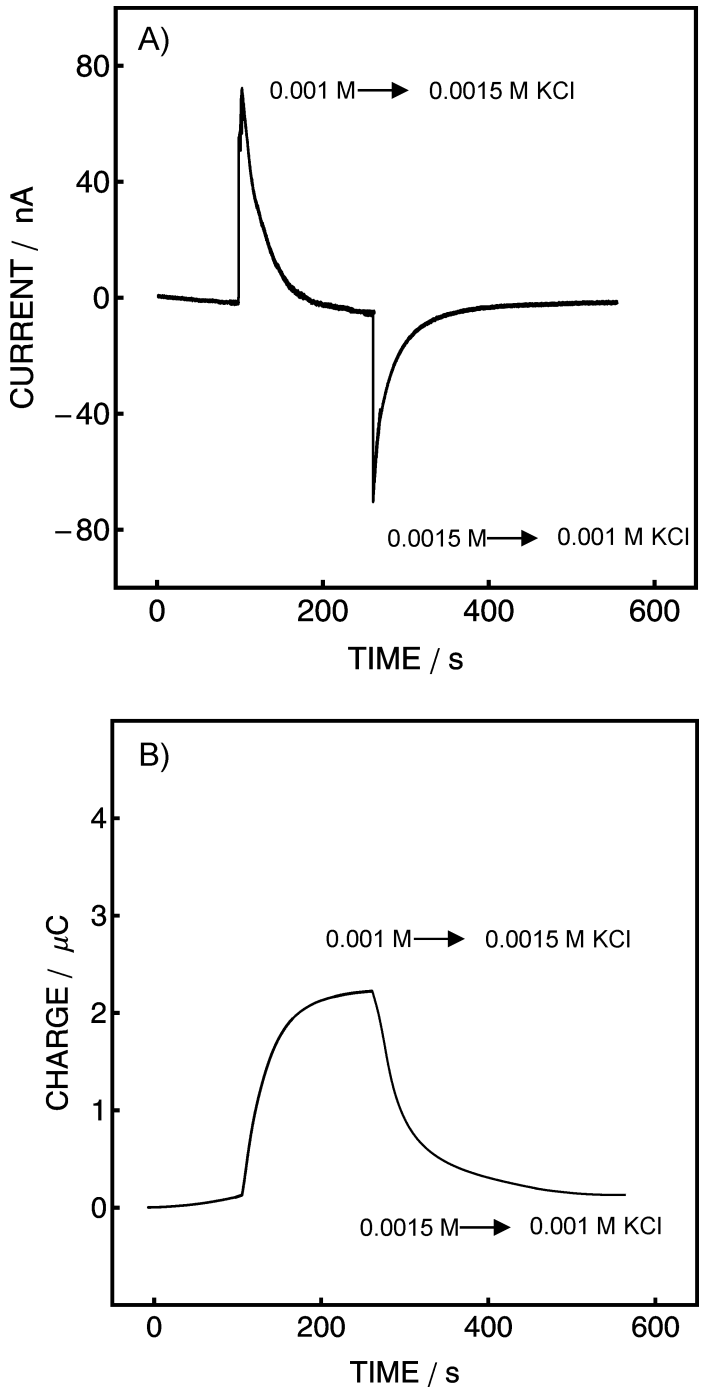

Figure S9 Reversible experimental current-time curves (A) and the corresponding charge-time curves (B) recorded for 10 mC of PEDOT(Cl) SC-ISE (M1).